Vietnam Journal of Science and Technology ***56*** *(1A) (2018) 14-24*

INVESTIGATION OF FABRICATION OF Co-Zr BASED RARE EARTH-FREE HARD MAGNETIC ALLOYS BY MELT-SPINNING METHOD

Nguyen Van Duong[1, 2, *], Nguyen Mau Lam[1], Duong Dinh Thang[1], Nguyen Huy Ngoc[3], Pham Thi Thanh[2, 4], Nguyen Hai Yen[2, 4], Do Bang[4], Luu Tien Hung[5], Nguyen Huy Dan[2, 4]

[1]*Hanoi Pedagogical University No 2, No 32 Nguyen Van Linh, Phuc Yen, Vinh Phuc, Viet Nam*

[2]*Graduate University of Science and Technology, VAST, No 18 Hoang Quoc Viet, Cau Giay, Ha Noi, Viet Nam*

[3]*VNU University of Engineering and Technology, No 144 Xuan Thuy, Cau Giay, Ha Noi, Viet Nam*

[4] *Institute of Materials Science, VAST, No 18 Hoang Quoc Viet, Cau Giay, Ha Noi, Viet Nam*

[5]*Nghean College of Education, No 389, Le Viet Thuat, Vinh, Nghe An, Viet Nam*

[*]Email*: duongnvsp2@gmail.com*

Received: 15 August 2017; Accepted for publication: 5 February 2018

ABSTRACT

Co-Zr based alloy has attracted much interest of potential to replace the rare earth-containing hard magnetic materials due to its high coercivity. In this study, we investigated the effects of subtituting elements of M (Ti, Si and Nb) and annealing temperature on the structure and magnetic properties of $Co_{79-x}Zr_{18+x-y}M_yB_3$ alloy ribbons (x = 0 - 2, y = 0 - 4). The alloy ribbons with a thickness of 20 µm were prepared by melt-spinning method with a rolling speed of 40 ms^{-1}. A part of the melt-spun ribbons was annealed at different temperatures from 550 to 800 ^oC for various durations from 2 to 15 minutes. Their structure and magnetic properties were investigated by X-ray diffraction (XRD) and a pulsed field magnetometer (PFM), respectively. The results of the XRD analysis showed that two soft magnetic phases, namely Co and $Co_{23}Zr_6$, coexist with a Co_5Zr hard magnetic phase in the alloy ribbons. The fraction of these phases was changed with both the concentration of the subtituting elements and annealing process. Hard magnetic properties of the alloy ribbons can be strengthened significantly, namely a large coercivity H_c > 4 kOe and maximum energy product $(BH)_{max}$ > 3.5 MGOe were obtained with an appropriate concentration of Ti, Si or Nb and annealing process. Furthermore, the subtituting elements also affect the optimal annealing temperature for these alloys. The obtained strong hard magnetic parameters of these rare earth-free alloys are of great importance in pratical application.

Keywords: hard magnetic materials, coercive force, rare earth-free hard magnetic materials, rapid quenching method.

1. INTRODUCTION

The rare earth-containing hard magnetic materials with their good intrinsic properties have been extensively used in common elecfonical devices from mobile phones and laptops to electric motors, generators, flywheel enerry storage, magnetic levitation transport, etc [l-2]. However, rare earth elements are becoming quickly exhausted in nature making the price of rare earth magnets increase rapidly [3]. Therefore, scientists have been focusing on finding out new hard magnetic materials which contain no rare earth elements and can be applied in practical applications. Recently, it has been reported that Co-Zr based alloys show promising magnetic properties including relative high magnetocrystalline anisotropy, high Curie temperature and high coercivity [4-7]. It is found that the $Co_{80}Zr_{18}B_2$ alloy ribbons, which are fabricated by using a rapid quenching method and consequently annealing, could have a coercivity (H_c) as high as of 4.4 kOe and maximum energy product $(BH)_{max}$ of 4.7 MGOe [7]. These hard magnetic properties in these alloys are attributed to the $Co_{11}Zr_2$ and Co_5Zr phases [6, 8-17]. There are several approaches to enhance the coercivity of Co-Zr based alloys, such as adding metallic elecments (Ti, Si or Mo) to facilitate the formation of the hard-magnetic phases and decrease both the grain size and the fraction of the soft magnetic phase of Co [18-22].

According to Gabai et al. [23], the replacement of Ti for Zr can prevent the development of gains in the $Co_{83.6}Zr_{16.4}$ alloy ribbons resulting in effectively changes of the magnetic properties of $Co_{80}Zr_{18-x}Ti_xB_2$ (x = 1, 2, 3 and 4) alloys. In particular, the values of coercivity H_c and maximum energy product $(BH)_{max}$ of these alloys were increased from 3 to 3.2 kOe and 3.2 to 5 MGOe, respectively, with x = 3 [24]. On the other hand, Chang et al. [22] showed that the replacement of Si for Zr also can improve the remanence B_r, coercivity H_c and maximum energy product $(BH)_{max}$ of $Co_{80}Zr_{18-x}Si_xB_2$ (x = 0 - 2) alloy ribbons. The optimal magnetic properties (B_r = 5.2 kG, H_c = 4.5 kOe and $(BH)_{max}$ = 5.3 MGOe) were obtained in $Co_{80}Zr_{17}Si_1B_2$ ribbons (x = 1). Furthermore, the highest H_c ~ 6.7 kOe was obtained for the $Co_{76}Zr_{18}Si_3B_3$ alloys after annealing at 500-700 ^oC for 5 - 20 minutes [4]. The effect of Nb substitution for Zr and annealing temperture on the structure and magnetic properties of $Co_{80}Zr_{18-x}Nb_xB_2$ (x = 1 - 4) alloy ribbons also has been investigated by Hou et al [25]. The highest value of H_c = 5.1 kOe and $(BH)_{max}$ = 3.4 MGOe were obtained by substituting 3 at% of Nb for Zr and annealing at 600 ^oC for 3 minutes. However, these hard magnetic properties are still lower than those of the rare earth-based alloys for the pratical applications.

In this paper, we present the effects of subtituting elements of M (Ti, Si and Nb) and annealing temperatures on the structure and magnetic properties of $Co_{79-x}Zr_{18+x-y}M_yB_3$ alloy ribbons (x = 0 - 2, y = 0 - 4). Hard magnetic properties of the alloy ribbons can be strengthened so significantly as a coercivity of H_c > 4 kOe and maximum energy product of $(BH)_{max}$ > 3.5 MGOe with an appropriate concentration of Ti, Si or Nb and annealing process.

2. EXPERIMENTAL

In this study, ingots with nominal compositions of $Co_{79-x}Zr_{18+x-y}M_yB_3$ (M = Ti, Si and Nb, x = 0 - 2, y = 0 - 4) were prepared from pure components of Co, Zr, Ti, Si, Nb and B using an arc-melting furnace to ensure their homogeneity. Then the melt-spun ribbons were fabricated by a single roller melt-spinning system. The ribbons of 2-mm-width and 20-µm-thick were obtained with a rolling speed of 40 ms^{-1}. A part of the melt-spun ribbons was annealed at various temperatures (550 – 800 ^oC) and durations (2 - 15 minutes). All the arc-melting, melt-spinning and annealing processes were performed under Ar atmosphere to avoid oxidization. The

structure and magnetic properties of the alloy ribbons were analyzed by X-ray diffraction (XRD) and a pulsed fleld magnetometer (PFM), respectively. The demagnetization effect, which depends on shape of measured specimens, was taken into account calculation of $(BH)_{max}$ of the alloys.

3. RESULTS AND DISCUSSION

3.1. Structure of the alloy ribbons

Figure 1 shows the XRD patterns of the $Co_{79-x}Zr_{18+x-y}M_yB_3$ (M = Ti, x = 0, y = 1 - 4) alloy ribbons before annealing (for y = 1, 2, 3 and 4) and after annealing (for y = 2) at T_a = 650 ^oC for t_a = 10 minutes.

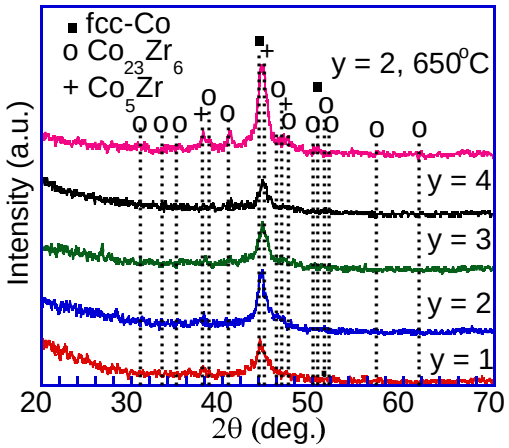

Figure 1. XRD patterns of the $Co_{79}Zr_{18-y}Ti_yB_3$ (y = 1 - 4) alloy ribbons before (for y = 1, 2, 3 and 4) and after (for y = 2) annealing at T_a = 650 ^oC for t_a = 10 minutes.

For the as-spun ribbons, only a large diffraction peak which is assigned to a soft magnetic phase of fcc-Co is observed while very small diffraction peaks of hard magnetic phase of Co_5Zr is shown. When the alloy ribbons were annealed at 650 ^oC for 10 minutes, the intensity of the diffraction peaks of the hard magnetic phase of Co-Zr is significantly increased, especially the Co_5Zr hard magnetic phase. On the other hand, the annealed alloy ribbon shows another $Co_{23}Zr_6$ soft magnetic phase. These obtained results are consistent with those of $Co_{80}Zr_{18}B_2$ alloy ribbons which are reported in Refs [6, 8, 26, 27].

Figure 2 shows the XRD patterns of Si-subtituting $Co_{79-x}Zr_{18+x-y}Si_yB_3$ (x = 2, y = 0 - 4) ribbons before and after annealing at 650^oC for 10 minutes. It is clearly seen that all the as-quenched ribbons already have crystalline phases which are assigned to fcc-Co, $Co_{23}Zr_6$ and Co_5Zr phases (Fig. 2a). However, some of these crystalline peaks have low intensity. This suggests that the as-quenched ribbons are not completely crystallized. On the other hand, for ribbons annealed at 650^oC for 10 minutes, the XRD peaks of the the annealed ribbons are similar to those of as-spun ribbons with y = 0, 2 and 4 but are strongly increased in the annealed ribbon with y = 3 (Fig. 2b).

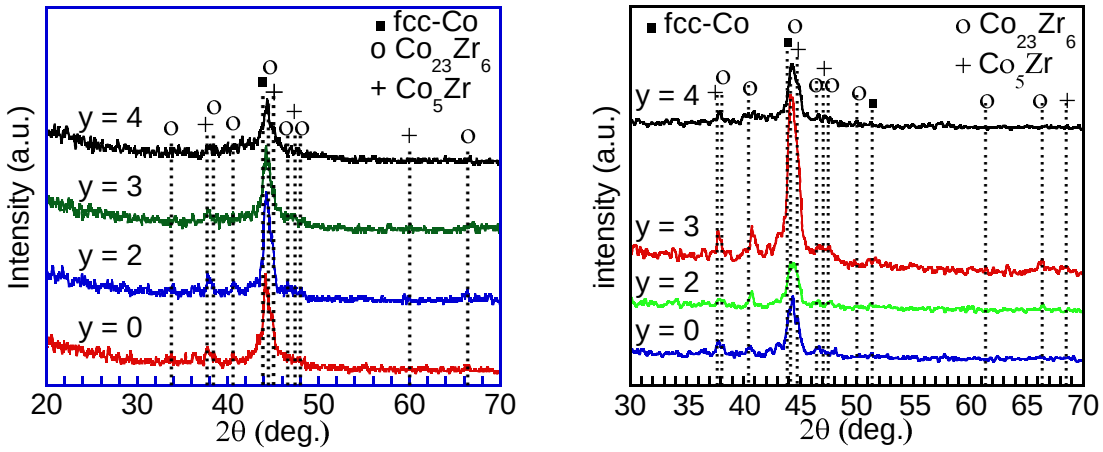

a) *b)*

Figure 2. XRD patterns of $Co_{77}Zr_{20-y}Si_yB_3$ (y = 0 - 4) ribbons before (a) and after (b) annealing at 650°C for 10 minutes.

The XRD patterns of the Nb-subtituting $Co_{79-x}Zr_{18+x-y}Nb_yB_3$ (x = 2, y = 0 - 4) ribbons before and after annealing at 650 °C for 15 minutes are shown in Fig. 3. It can be seen that, the structure of the as-spun alloy ribbons shows the both soft magnetic phase of fcc-Co and hard magnetic phase of Co_5Zr (Fig. 3a). However, by annealing, difraction pattems of the alloy ribbons appear more peaks corresponding to $Co_{23}Zr_6$ soft magnetic phase (Fig. 3b).

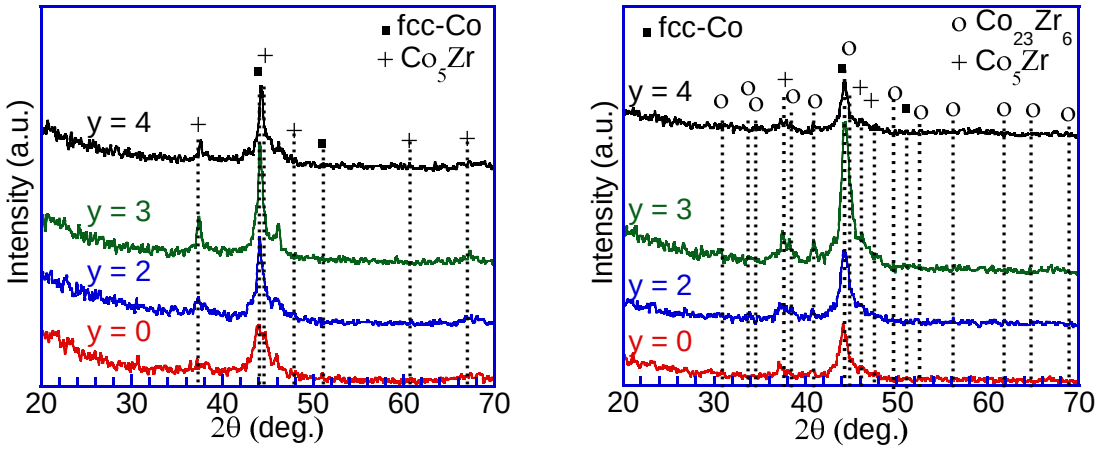

a) *b)*

Figure 3. XRD patterns of $Co_{77}Zr_{20-y}Nb_yB_3$ (y = 0 - 4) ribbons before (a) and after annealing at 650 °C for 15 minutes (b).

3.2. Magnetic properties of the alloy ribbons

The hysteresis loops of the $Co_{79-x}Zr_{18+x-y}M_yB_3$, (M = Ti, Si and Nb) as-spun ribbons are shown in Fig. 4. The results show that all the alloy ribbons have hard magnetic properties. However, their coercivities are rather small and less than 2.48 kOe. It should be noted that their coercivities are slightly increased from 2.21 to 2.25 kOe with a small change of the Ti concentration from 1 to 2 at%, and then reaches the highest value of 2.48 kOe with the Ti concentration of 3 at% (Fig. 4a). When the Ti concentration is further increased up to 4 at%, the coercivity is quickly decreased to 1.32 kOe. For the Si-subtitting $Co_{79-x}Zr_{18+x-y}Si_yB_3$ (x = 2, y = 0

- 4) as-quenched ribbons, their coercivities are also increased from 3.26 to 3.95 kOe when the Si concentration is increased from 0 to 2 at% and then is quickly decreased to 2.1 kOe with further increasing of the Si concentration up to 4 at% (Fig. 4b).

This result can be explained by the change of the Co_5Zr hard magnetic phase fraction, which increases with increasing the Ti concentration from 0 to 3 at% and then decreases with further increasing the Ti concentration up to 4 at% as shown in Fig. 1 and Fig. 2a.

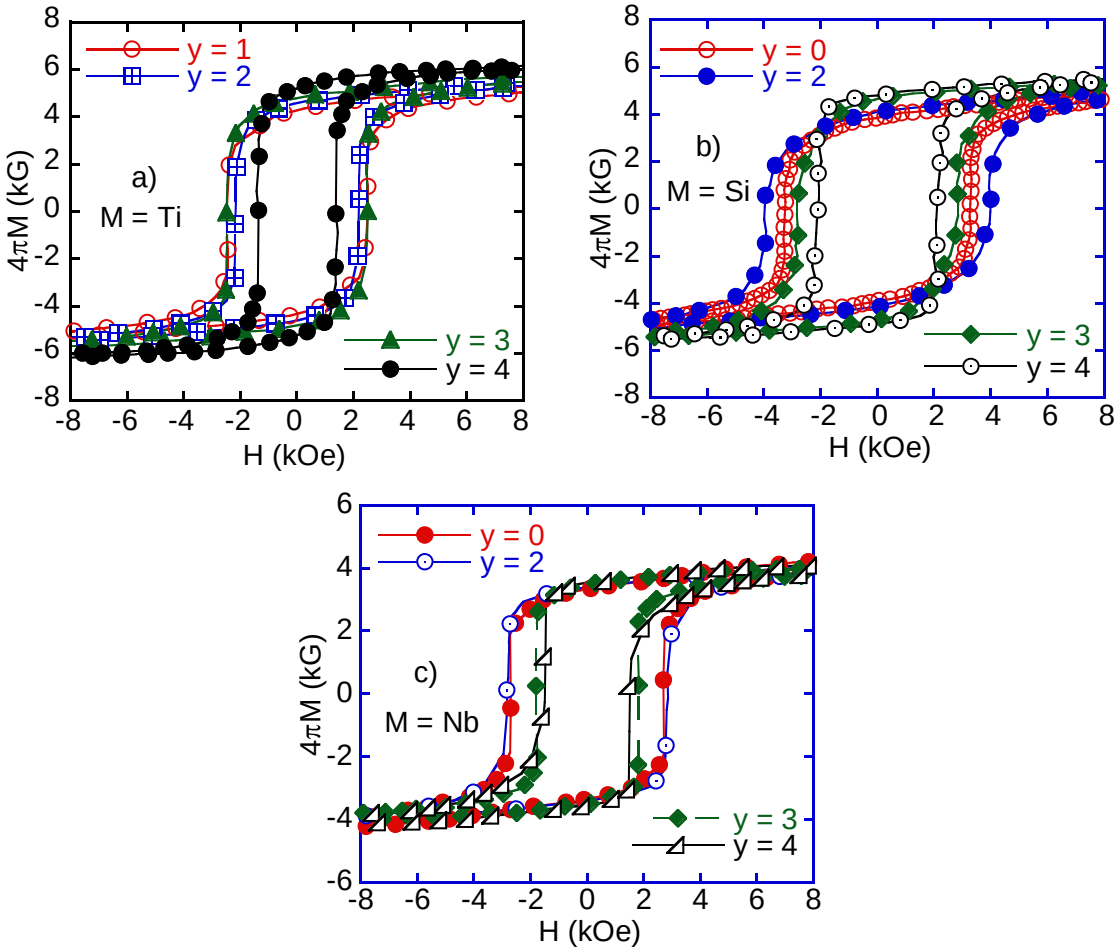

Figure 4. Hysteresis loops of $Co_{79-x}Zr_{18+x-y}M_yB_3$ as-quenched ribbons with M = Ti (a) (x = 0); M = Si (b) (x = 2); M = Nb (c) (x = 2).

For the Nb-subtituting $Co_{79-x}Zr_{18+x-y}Nb_yB_3$ (x = 2 and y = 0 - 4) as-spun ribbons, similar to those of the Ti and Si-subtituting alloy ribbons, their coercivities are first slightly increased from 2.68 kOe (y = 0) to 2.83 kOe (y = 2) and are then strongly decreased to 1.32 kOe when the Nb concentration is increased up to 4 at%.

To find the tendency of changing coecivity H_c of the $Co_{79-x}Zr_{18+x-y}M_yB_3$ (M = Ti, Si, Nb, x = 0 - 2, y = 0 - 4) as-spun alloy ribbons, we summaried its dependence on the concentration of the subtituting elements as shown in Fig. 5. The result shows that, the optimal substituting concentration and the maximal H_c are different for subtituting elements. The subtitution of Si for Zr is most effective to improve the coecivity of the as-spun ribbons.

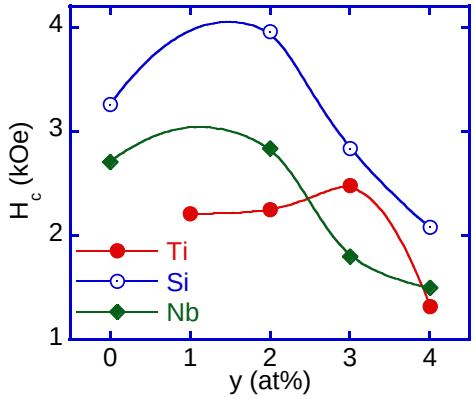

Figure 5. Dependence of coercivity on the concentration of the doping elements of the $Co_{79-x}Zr_{18+x-y}M_yB_3$ (M = Ti, Si, Nb, x = 0 - 2, y = 0 - 4) as-spun ribbons.

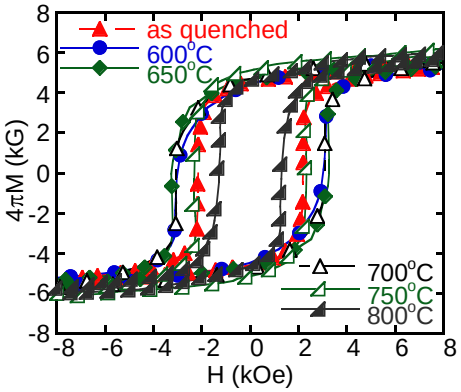

Figure 6. Hysteresis loops of $Co_{79}Zr_{16}Ti_2B_3$ melt-spun ribbons before annealing and annealing at various temperatures for 10 minutes.

In order to investigate the effect of the annealing process, we annealed the as-spun ribbons at different temperatures from 500 to 800 °C for various durations from 2 to 15 minutes. Figure 6 shows the hysteresis loops of the $Co_{79}Zr_{16}Ti_2B_3$ alloy ribbons before and after annealing at the temperatures of 600, 650, 700, 750 and 800 °C for 10 minutes. The results show that the coercivity of the annealed alloy is strongly increased with increasing the annealing temperature to 650 °C and then is decreased with further increasing the annealing temperature up to 800 °C.

Figure 7 shows the hysteresis loops of the $Co_{79-x}Zr_{18+x-y}M_yB_3$ (M = Si and Nb, x = 2, y = 0 - 4) ribbons after annealing at 650 °C for 10 - 15 minutes. We also summaried the dependence of the H_c on the annealing temperture of the annealed ribbons as shown in Fig. 8 to find the tendency of changing coecivity H_c of the $Co_{79-x}Zr_{18+x-y}M_yB_3$ (M = Si and Nb, x = 2, y = 0 - 4) alloy ribbons after annealing. The dependence of the coercivity H_c on annealing temperature of the Ti-subtituting $Co_{79}Zr_{18-y}Ti_yB_3$ (y = 1, 2, 3 and 4) alloy ribbons annealed for 10 minutes is shown in Fig. 8a. One can see that when the alloyribbons are annealed at temperatures from 500 to 650 °C, their coercivity H_c and maximumenergy product $(BH)_{max}$ are in creased up to their maximum values of 3.45 kOe and 3.47 MGOe, respectively. It can be explained that when Ti subtitutes for Zr, a part of Ti atoms penetrating into the lattice of $Co_{23}Zr_6$ and Co_5Zr phases causes a change the electronic structure of 3d subshell [28]. However, when the annealing temperature is further increased from 650 to 800 °C, the coercivity H_c and maximum energy product $(BH)_{max}$ of the alloys are drastically decreased. These changes can be attributed to the

change of the volume fractions of the Co and $Co_{23}Zr_6$ soft magnetic phases and the Co_5Zr hard magnetic phase due to the decomposition of the magnetic hard phase into magnetically soft phases. This decomposition has been investigated for both the Co-Zr and Co-Zr-B alloys at the temperature of 800 ^oC as reported in Refs. [8, 29, 30].

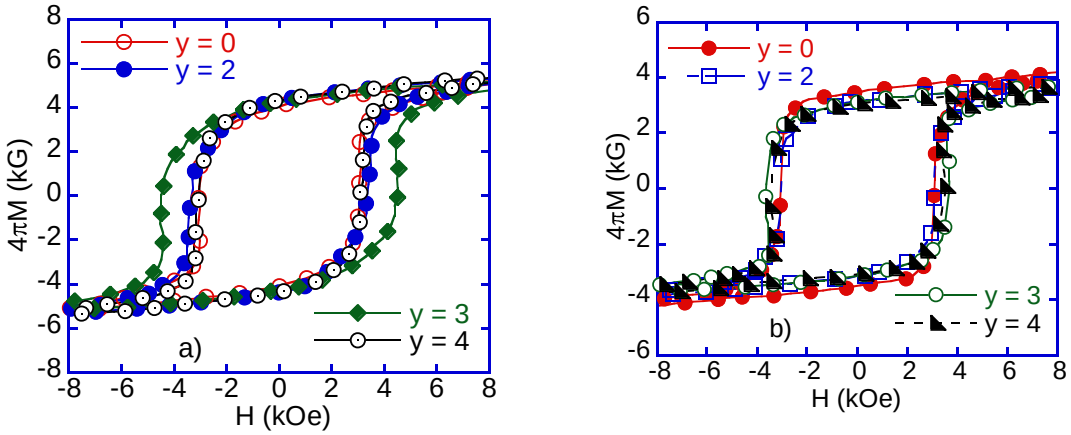

Figure 7. Hysteresis loops of (a) $Co_{77}Zr_{20-y}Si_yB_3$ (y = 0 - 4) ribbons annealed at 650 ^oC for 10 minutes and (b) $Co_{77}Zr_{20-y}Nb_yB_3$ (y = 0 - 4) ribbons annealed at 650 ^oC for 15 minutes.

On the other hand, the annealing temperature dependence of the coercivity for different Si concentrations of y = 0 - 4 is shown in Fig. 8b. The highest coercivity of 4.5 kOe was obtained for the ribbon subtituted with 3 at% of Si and annealed at 650 ^oC for l0 minutes. Figure 8c shows the dependence of the coercivity H_c on annealing temperature of the $Co_{77}Zr_{20-y}Nb_yB_3$ (y = 0, 2, 3 and 4) alloy ribbons annealed at 650 ^oC for 15 minutes. It is found that, the coercivity H_c is first increased when the annealing temperature increases from 550 to 650 ^oC then it is drastically decreased with further increasing the annealing temperature up to 700 ^oC. The highest coercivity of 3.71 kOe was obtained for the alloy ribbons subtituted with 3 at% of Nb and annealed at 650 ^oC for 15 minutes.

The annealing temperature dependence of the maximum energy product $(BH)_{max}$ of the $Co_{79-x}Zr_{18+x-y}M_yB_3$ (M = Ti, Si, Nb, x = 0 - 2; y = 0 - 4) annealed ribbons is shown in Fig. 9. The results show that, the maximum energy product $(BH)_{max}$ reached optimal values when the annealing temperature is in range of 650 - 700 °C. With the Ti subtitution, the maximum energy product $(BH)_{max}$ ~3.47 MGOe was obtained with 2 at% of Ti and the annealing temperature of 650 ^oC for 10 minutes. Meanwhile, $(BH)_{max}$ ~ 3.53 MGOe and 1.5 MGOe were obtained with 3 at% substitution of Si and Nb for Zr and the annealing temperature of 650 ^oC for 10 minutes and 15 minutes, respectively. These enhancements of the coercivity and maximum energy product can be attributed to the exchange coupling which is strengthened due to the appropriate reduction of grain size. However, the grain size is significantly increased and further different from the optimal size at the higher annealing temperatures [26].

The optimal magnetic properties of $Co_{79-x}Zr_{18+x-y}M_yB_3$ (M = Ti, Si, Nb, x = 0 - 2; y = 0 - 4) annealed alloy ribbons are summaried and shown in Table 1. It can be seen that, the concentration of subtituting elements and the annealing temperture significantly affected on the magnetic properties of the alloy ribbons. The optimal results are comparable with those of $Co_{80}Zr_{17}Si_1B_2$ ribbons which are reported by Chang et al. in Ref. [22].

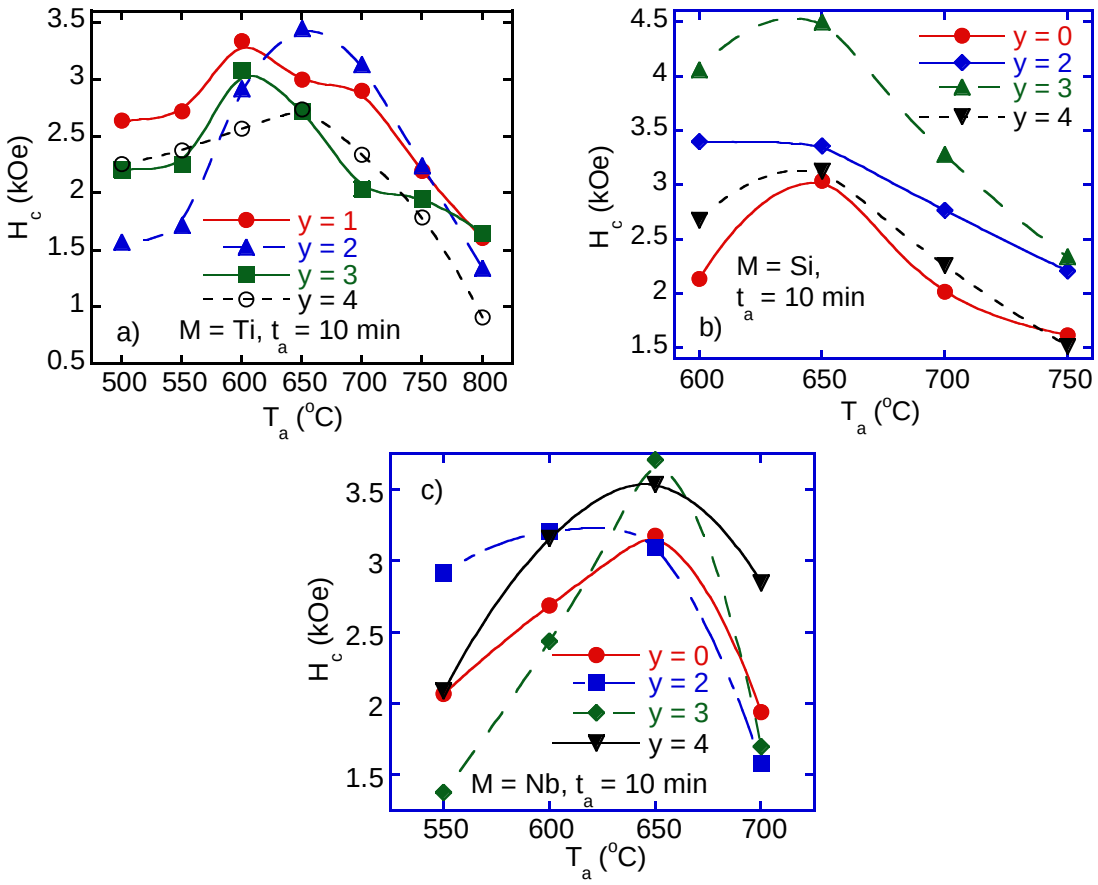

Figure 8. Dependence of coercivity H_c on annealing temperature of (a) $Co_{79}Zr_{18-y}Ti_yB_3$ (y = 1 - 4); (b) $Co_{77}Zr_{20-y}Si_yB_3$ (y = 0 - 4); $Co_{77}Zr_{20-y}Nb_yB_3$ (y = 0 - 4) ribbons annealed at various temperatures T_a for time t_a of 10 - 15 minutes.

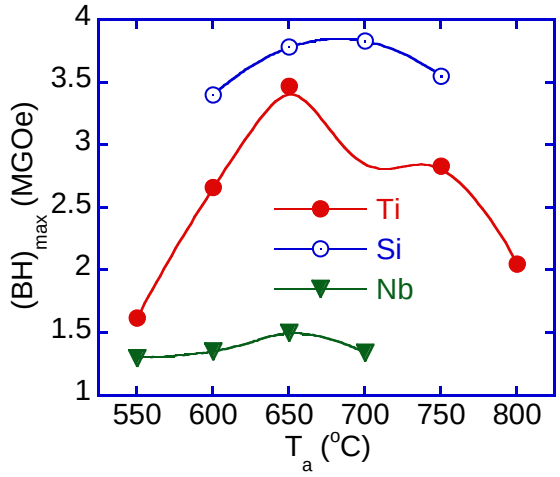

Figure 9. The dependence of maximum energy product $(BH)_{max}$ on the annealing temperature of the $Co_{79-x}Zr_{18+x-y}M_yB_3$ (M = Ti, Si, Nb, x = 0 - 2, y = 0 - 4) ribbons annealed at various temperatures for 10 - 15 minutes.

Table 1. Optimal magnetic properties of $Co_{79-x}Zr_{18+x-y}M_yB_3$ (M = Ti, Si, Nb, x = 0 - 2; y = 0 - 4) annealed alloy ribbons.

Composition	T_a (^{o}C)	t_a (minutes)	M_s (emu/g)	M_r (emu/g)	B_r (kG)	H_c (kOe)	$(BH)_{max}$ (MGOe)
$Co_{79}Zr_{16}Ti_2B_3$	650	10	68	49.18	4.69	3.45	3.47
$Co_{77}Zr_{17}Si_3B_3$	650	10	73	44.63	4.26	4.50	3.53
$Co_{77}Zr_{17}Nb_3B_3$	650	15	46	32.84	3.13	3.71	1.50

4. CONCLUSION

The $Co_{79-x}Zr_{18+x-y}M_yB_3$ (M = Ti, Si, Nb, x = 0 - 2; y = 0 - 4) alloy ribbons were fabricated by melt-spinning method and annealed at different conditions. Concentration of subtituted elements and annealing temperature strongly influence on the structure and magnetic properties of the alloy ribbons. The structure of the alloy ribbons mainly consists of two magnetic soft phases of Co and $Co_{23}Zr_6$ and a hard magnetic phase of Co_5Zr. By optimizing the concentration of substituting Ti, Si or Nb elements and annealing process, hard magnetic properties of alloy ribbons are strengthened significantly. In particular, remanence B_r = 4.26 kG, coecivity H_c = 4.5 kOe and maximum energy product $(BH)_{max}$ = 3.53 MGOe were obtained in $Co_{77}Zr_{17}Si_3B_3$ alloy ribbons annealed at 650 ^{o}C for 10 minutes.

Acknowledgement. This work was supported by the science and technology project of Hanoi Pedagogical University 2, code: C.2018.10. This work was implemented at the Key Laboratory of Electronic Materials and Devices, Institute of Materials Science, Vietnam Academy of Science and Technology. A part of work was done at the Laboratory of Faculty of Physics, Hanoi Pedagogical University No 2.

REFERENCES

1. Gutfleisch O., Willard M. A., Bruck E., Chen C. H. and Sankar S. G. - Magnetic Materials and Devices for the 21st Century: Stronger, Lighter, and More Energy Efficient, Adv. Mater. **23** (2011) 821-842.
2. Li D., Pan D., Li S. and Zhang Z. - Recent developments of rare-earth-free hard-magnetic materials, Sci. China-Phys. Mech. Astron. **59** (1) (2016) 617501-1- 617501-17.
3. Bourzac K. - The rare-earth crisis, Technol. Rev. **114** (2011) 58-63.
4. Gao C., Wan H. and Hadjipanayis G. C. - High coercivity in non-rare-earth containing alloys, J. Appl. Phys. **67** (1990) 4960-4962.
5. Ghemawat A. M., Foldeaki M., Dunlap R. A. and O'Handley R. C. - New microcrystalline hard magnets in a Co-Zr-B alloy system, IEEE Trans. Magn. **25** (1989) 3312-3314.
6. Ishikawa T. and Ohmori K. - Hard magnetic phase in rapidly quenched Zr-Co-B alloys, IEEE Trans. Magn. **26** (1990) 1370-1372.
7. Saito T. - High performance Co-Zr-B melt-spun ribbons, Appl. Phys. Lett. **82** (14) (2003) 2305-2307.
8. Stadelmaier H. H., Jang T. S. and Henig E. Th. - What is responsible for the magnetic hardness in Co-Zr(-B) alloys?, Mater. Lett. **12** (1991) 295-300.

9. Stadelmaier H. H. and Henig E. Th. - Permanent magnet materials-Developments during the past 12 months, J. Mater. Eng. Perform. **1** (1992) 167-174.
10. Gabay A. M., Zhang Y. and Hadjipanayis G. C. - Cobalt-rich magnetic phases in Zr-Co alloys, J. Magn. Magn. Mater. **236** (2001) 37-41.
11. Ivanova G. V., Shchegoleva N. N. and Gabay A. M. - Crystal structure of Zr_2Co_{11} hard magnetic compound, J. Alloys Compd. **432** (2007) 135-141.
12. Saito T. and Itakura M. - Microstructures of Co-Zr-B alloys produced by melt-spinning technique, J. Alloys Compd. **572** (2013) 124-128.
13. Stroink G., Stadnik Z. M., Viau G. and Dunlap R. A. - J. Appl. Phys. **67** (1990) 4963-4965.
14. Burzo E., Grossinger R., Hundegger P., Kirchmayr H. R., Krewenka R., Mayerhofer O. and Lemaire R. - Magnetic properties of $ZrCo_{5.1-x}Fe_x$ Alloys, J. Appl. Phys. **70** (10) (1991) 6550.
15. Ivanova G. V. and Shchegoleva N. N. - The microstructure of a magnetically hard Zr_2Co_{11} alloy, Phys. Met. Metall. **107** (3) (2009) 270-275.
16. Zhang W. Y., Valloppilly S. R., Li X. Z., Skomski R., Shield J. E. and Sellmyer D. J. - Coercivity enhancement in Zr_2Co_{11}-based nanocrystalline materials due to Mo addition, IEEE Trans. Magn. **48** (11) (2012) 3603-3605.
17. Balasubramanian B., Das B., Skomski R., Zhang W. Y. and Sellmyer D. J. - Novel nanostructured rare-earth-free magnetic materials with high energy products, Adv. Mater. **25** (42) (2013) 6090.
18. Jin Y. L., Zhang W. Y., Skomski R., Valloppilly S., Shield J. E. and Sellmyer D. J. - Phase composition and nanostructure of Zr_2Co_{11}-based alloys, J. Appl. Phys. **115** (17) (2014) 739-1-739-3.
19. Jin Y., Zhang W., Kharel P. R., Valloppilly S. R., Skomski R. and Sellmyer D. J. - Effect of boron doping on nanostructure and magnetism of rapidly quenched Zr_2Co_{11}-based alloys, AIP Advances **6** (2016) 056002-1-056002-5
20. Zhang W. Y., Valloppilly S., Li X. Z., Liu Y., Michalski S., George T. A., Skomski R. and Sellmyer D. J. - Magnetic hardening of Zr_2Co_{11}:(Ti, Si) nanomaterials, J. Alloys Compd. **587** (2014) 578-581.
21. Hou Z., Wang W., Xu S., Zhang J., Wu C. and Su F. - Hard magnetic properties of melt-spun $Co_{82}Zr_{18-x}Ti_x$ alloys, Physica B: Condens. Matter. **407** (7) (2012) 1047-1050.
22. Chang H. W., Tsai C. F., Hsieh C. C., Shih C. W., Chang W. C. and Shaw C. C. - Magnetic properties enhancement of melt spun CoZrB ribbons by elemental Substitutions, J. Magn. Magn. Mater. **346** (2013) 74-77.
23. Gabai A. M., Schegolewa N. N., Gaviko V. S. and Ivanova G. V. - Effect of component substitution on the magnetic properties of Zr_2Co_{11} phase and rapidly quenched Zr_2Co_{11}-based alloys, Phys Met. Metall. **95** (2003) 122-128.
24. Hou Z., Xu S., Zhang J., Wu C., Liu D., Su F. and Wang W. - High performance $Co_{80}Zr_{15}Ti_3B_2$ melt-spun ribbons, JAC. **555** (2013) 28-32.
25. Hou Z., Zhang J., Xu S., Wu C., Zhang J., Wang Z., Yang K., Wang W., Du X. and Su F. - Effects of Nb substitution for Zr on the phases, microstructure and magnetic properties of $Co_{80}Zr_{18-x}Nb_xB_2$ melt-spun ribbons, J. Magn. Magn. Mater. **324** (2012) 2771-2775.

26. Stroink G., Stadnik Z. M., Viau G. and Dunlap R. A. - The influence of quenching rate on the magnetic properties of microcrystalline alloys $Co_{80}Zr_{20-x}B_x$, J. Appl. Phys. **67** (1990) 4963-4965.

27. Saito T. - Magnetization process in Co-Zr-B permanent-magnet materials, IEEE Trans. Magn. **40** (4) (2004) 2919-2921.

28. Shen B., Yang L., Cao L. and Guo H. - Hard Magnetic properties in melt-spun $Co_{82-x}Fe_xZr_{18}$ alloys, J. Appl. Phys. **73** (1993) 5932-5934.

29. Cheng S. F., Wallace W. E. and Demczyk B. G. - Proceedings of the 6th International symposium on magnetic anisotropy an coercivity in rare-earth-transition-metal alloys. October 1990, Pittsburgh, PA, Carnegie-Mellon University, Pittsburgh, PA, (1991) 477.

30. Buschow K. H. J., Wernick J. H. and Chin G. Y. - Note on the Hf-Co phase diagram, J. Less Common Met. **59** (1978) 61.